Full empirical potential curves for the $X^1\Sigma^+$ and $A^1\Pi$ states of CH^+ from a direct-potential-fit analysis

Young-Sang Cho and Robert J. Le Roy
Department of Chemistry, University of Waterloo, Waterloo, Ontario N2L 3G1, Canada

(Received 23 October 2015; accepted 20 December 2015; published online 13 January 2016)

All available "conventional" absorption/emission spectroscopic data have been combined with photodissociation data and translational spectroscopy data in a global analysis that yields analytic potential energy and Born-Oppenheimer breakdown functions for the $X^1\Sigma^+$ and $A^1\Pi$ states of CH^+ and its isotopologues that reproduce all of the data (on average) within their assigned uncertainties. For the ground $X^1\Sigma^+$ state, this fully quantum mechanical "Direct-Potential-Fit" analysis yielded an improved empirical well depth of $\mathfrak{D}_e = 34\,362.8(3)$ cm^{-1} and equilibrium bond length of $r_e = 1.128\,462\,5\,(58)$ Å. For the $A^1\Pi$ state, the resulting well depth and equilibrium bond length are $\mathfrak{D}_e = 10\,303.7(3)$ cm^{-1} and $r_e = 1.235\,896\,(14)$ Å, while the electronic isotope shift from the hydride to the deuteride is $\Delta T_e = -5.99(\pm 0.08)$ cm^{-1}. © *2016 AIP Publishing LLC*. [http://dx.doi.org/10.1063/1.4939274]

I. INTRODUCTION

The methylidyne cation, CH^+, has been the subject of experimental and theoretical study for over 70 years. It was first identified as a species in interstellar space in 1941 when Douglas and Herzberg[1] generated laboratory spectra that allowed them to assign three previously observed interstellar lines[2–9] as $R(0)$ lines in bands of the $A(^1\Pi) - X(^1\Sigma^+)$ system of CH^+. This species is an important intermediate in combustion processes and atmospheric chemistry and is believed to play a crucial part in the chemistry of interstellar clouds.[10,11] It therefore became the subject of investigations to obtain information about its creation, destruction, and abundance in interstellar space, and astronomical observations have been followed by numerous laboratory studies.[11–33]

It is well understood that the most comprehensive and compact way of summarizing what we know about a given molecular species is by determining accurate potential energy functions for it. For many years, this was done by fitting experimental data to Dunham-expansion expressions for the vibration-rotational level energies[34,35] and then using the first-order semiclassical RKR method[36,37] to generate pointwise potential energy curves (PECs). However, this approach offers no natural way of extrapolating (or interpolating) to make realistic predictions in regions where there are no data, and the fact that the RKR method is not fully quantum mechanical limits its accuracy, particularly for small-reduced-mass species such as hydrides. Moreover, in this approach, it was impossible (or at least extremely difficult) to take account of and distinguish between higher-order semiclassical corrections and Born-Oppenheimer breakdown (BOB) effects. As a result, an increasingly widely used procedure today is the "direct-potential-fit" (DPF) methodology, in which least-squares fits of experiment data to synthetic spectra generated by exact quantum mechanical calculations from some trial analytic model for the potential energy function and relevant BOB corrections are used to optimize the parameters defining those trial functions. While the earliest application of a full DPF procedure (albeit not under that name) was for determining 3D potential energy surfaces,[38] its application to diatomic molecules seems to have originated with the development of what was called the "Inverse Perturbation Analysis" or IPA method of Kosman and Hinze[39] and Vidal and Scheingraber,[40] in which iterative application of first-order perturbation theory corrections yielded analytic functions correcting some preliminary estimate of a potential energy function, usually a set of first-order semiclassical RKR points. This was certainly a DPF-*type* procedure, except that it involved fitting to determine an analytic function *correcting* the preliminary pointwise potential, rather than the potential function itself, and the resulting PECs both lacked high-order continuity and incorporated no natural procedure for extrapolating inward or outward outside the preliminary "primitive" model region. The modern fully quantum-mechanical DPF methodology was developed by a number of groups in the early 1990's,[41–43] but the most successful general application fully incorporating BOB correction functions was the work of Coxon and co-workers,[41,44] while analogous work from other laboratories proceeded soon afterwards.[45–48] Although its authors called it an IPA method, the work of Pashov and co-workers[49–51] is also a true DPF procedure, in that their cubic spline through a chosen set of points with the potential energies at the selected cubic spline points being the parameters defining their PECs provides a unified analytic model for the potential function itself and not for a correction to add to some starting potential.

To date, all analyses of the "conventional" data for the methylidyne cation system have consisted of traditional band-constant or Dunham-expansion fits to the data for the lower vibrational levels of the two states,[52] and there had been no systematic effort to merge the data for the various isotopologues in a single analysis. Moreover, while there have been a number of innovative studies of high-J and high-v predissociating states,[17,18,23,26,30] their analyses mostly involved coupled-channel bound → continuum simulations of

 © 2016 AIP Publishing LLC

This article is copyrighted as indicated in the article. Reuse of AIP content is subject to the terms at: http://scitation.aip.org/termsconditions. Downloaded to IP: 129.97.80.15 On: Wed, 13 Jan 2016 18:34:46

the predissociation spectra using (at best) poorly specified combinations of segments of *ab initio*, long-range, and empirical functions. Furthermore, no fully satisfactory treatment has combined them with the "conventional" low-$\{v, J\}$ transition energy data in a single quantitative analysis. The present work addressed this situation by performing a fully quantum mechanical DPF analysis[53] that determines full analytic potential energy and Born Oppenheimer breakdown functions for the $X^1\Sigma^+$ and $A^1\Pi$ states of CH^+ that are able to account for all of the available data (on average) within their uncertainties. In place of relatively complicated scattering and/or coupled-channel calculations for the upper levels of the photodissociation transitions, we locate the observed "quasibound" tunneling-predissociation levels using the "Airy function third-turning-point boundary condition" that has been shown to be accurate to within a small fraction of the tunneling width,[54,55] while the Feshbach-predissociating high-v levels of the $A^1\Pi$ state are defined simply as truly bound levels of our 1-D model potential function for this state. This approach neglects the small level shifts associated with coupling to or between continuum states, but we do not believe that this introduces significant errors, and the resulting potential energy functions provide a compact and easily portable summary of our knowledge of these species.

II. DATA USED IN THE ANALYSIS

A. "Conventional" transition-energy data

An overview of the data for the $A^1\Pi - X^1\Sigma^+$ system of CH^+ is presented in Table I, while the vibrational level energies seen in Fig. 1 indicate the range of the conventional transition-energy data used in this study. Following Douglas and Herzberg's original report[1] that four observed interstellar absorption lines belonged to CH^+, they presented details of their laboratory measurement of four emission bands that they identified as the (0–0, 1–0, 2–0, 0–1) bands of the $A^1\Pi - X^1\Sigma^+$ system of CH^+ and showed that the $R(0)$ lines of the first three bands agree with the three of four observed molecular interstellar absorption lines (those at λ = 4232.58, 3957.72, 3745.33 Å).[12] Their reported wavelength uncertainty of ±0.01 Å corresponds to wavenumber uncertainties of 0.06–0.08 cm^{-1}. Two decades later Douglas and Morton extended this study to include the 0–1, 1–1, 2–1, 3–1, and 4–1 emission bands[13] and reported that their calculated position for the $R(0)$ line of the unobserved 3–0 band agrees with the fourth of the interstellar absorption lines reported by Adams[9] (the one at λ = 3579.04 Å).[13] They did not report uncertainties for their data,[13] and ±0.02 cm^{-1} has been used here. After another two decade gap, Grieman *et al.*[11] reported the observation of a number of new higher-J lines in the 0–0 band of CH^+ and of the 0–0 and 2–1 bands of CD^+, but their precision was relatively modest, and their 2–1 CD^+ band data was excluded here because it was incompatible with the much higher resolution data of Bembenek *et al.*[22] A year later, the first high-resolution (±0.007–0.01 cm^{-1}) data for this species were reported by Carrington and Ramsey,[19] who analyzed eight bands of the $A^1\Pi - X^1\Sigma^+$ system that involved $v'(A)$ = 0–3 and $v''(X)$ = 0–3 and provided the first observation of levels $v''(X)$ = 2 and 3. Finally, the most recent "conventional" electronic spectroscopy investigation of $^{12}CH^+$ was that of Hakalla *et al.*,[29] who reported new measurements

TABLE I. Overview of the data used in this analysis.

Isotope	$v(A)$	$v(X)$	J	uncertainty (cm^{-1})	No. data	Reference
$^{12}CH^+$	0–2	0–1	0–11	0.06–0.08	94	Douglas[12]
	0–4	1	0–16	0.02	127	Douglas[13]
	0	0	5–21	0.5	35	Grieman *et al.*[11]
	0–3	0–3	0–15	0.007–0.01	231	Carrington[19]
	0–9	0–5	14–35	3.0	47[a]	Helm[18]
	...	0–10	12–35	20.0–152.4	32[a,b]	Helm[18]
	0–2	1	31–35	1.0	6[a]	Sarre[23]
	11–14	0	0–9	0.4–9.0	34[c]	Hechtfischer[26]
	...	$\mathfrak{D}_0(X)$	0	0.11	1	Hechtfischer[26]
	...	0	1–6	0.01–0.08	6[d]	Cernicharo[97]
	0, 2	0–1	0–17	0.005–0.018	119	Hakalla[29]
	...	0	0–3	$7\times10^{-7}-3.3\times10^{-6}$	3[d]	Yu[33]
$^{12}CD^+$	0–3	0–1	0–12	*Not included*	152	Antić-Jovanović[16]
	0	0	8–23	0.5	24	Grieman[11]
	0–3	0–3	0–14	0.004–0.03	258	Bembenek[22]
	...	0	0–4	$7\times10^{-7}-3.3\times10^{-6}$	4[d]	Yu[33]
$^{13}CH^+$	3	1	1–4	0.02	4	Antić-Jovanović[20]
	0–2	1	31–35	1.0	6[a]	Sarre[23]
	0–2	0–1	0–12	0.008	141	Bembenek[24]
	...	0	0–3	$1\times10^{-6}-3.3\times10^{-6}$	3[d]	Yu[33]
$^{13}CD^+$	0–1	0	0–1	0.004–0.006	83	Bembenek[25]

[a]Shape resonances.
[b]Fragment kinetic energies.
[c]Feshbach resonances.
[d]Microwave data.

This article is copyrighted as indicated in the article. Reuse of AIP content is subject to the terms at: http://scitation.aip.org/termsconditions. Downloaded to IP: 129.97.80.15 On: Wed, 13 Jan 2016 18:34:46

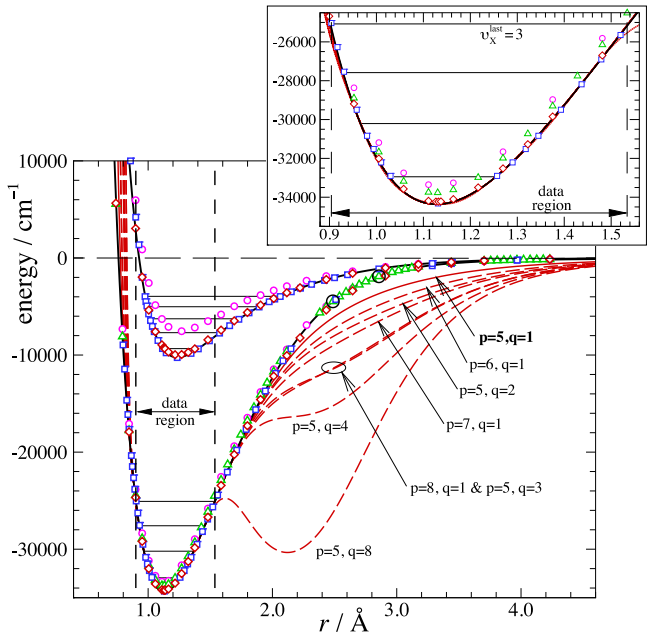

FIG. 1. Overview of the present study of the $A^1\Pi$ (upper curves and points) and $X^1\Sigma^+$ (lower curves and points) states of CH^+. Horizontal black lines indicate the levels $v(X) = 0$–3 and $v(A) = 0$–4 observed by "conventional" spectroscopy,[11–13,19] while the dashed red curves are the results of X-state-alone fits using a variety of choices for the exponent-variable parameters p and q, leading to the optimum purely "data-only" $\{p, q\} = \{5, 1\}X$-state solid red curve. The small open points are the *ab initio* results of Saxon *et al.*[78] (purple circles), of Sauer and Špirko[79] (green delta's), and of Biglari *et al.*[80] (red diamonds), while the blue squares are the semi-empirical PEC points of Sarre[23] and the solid black curves shows the final recommended X and A-state potentials obtained from our full two-state multi-isotopologue DPF analysis while including the two *ab initio* X-state points identified with large open black rings as pseudo-data on the fits.

of the 0–0, 0–1, and 2–1 bands of $A^1\Pi - X^1\Sigma^+$ system at high resolution.

The first pure rotational data for $^{12}CH^+$ were obtained by Cernicharo *et al.*[56] who observed the far-infrared $R(1)$–$R(5)$ transitions in the spectrum of a planetary nebula at relatively low resolution. A decade later, direct laboratory measurements of the $R(0)$ transition of $^{12}CH^+$ were reported by Falgarone *et al.*[27] and by Pearson and Drouin,[28] but they were later superseded by the much more precise laboratory measurements of the $R(0)$–$R(3)$ lines of $^{12}CH^+$, $^{13}CH^+$, and $^{12}CD^+$ by Amano and co-workers,[31,33] which combine to give an extremely accurate measure of the locations of the potential minima.

The first definitive observations of any of the minor carbon isotopologues of CH^+ were the 1979 report by Antić-Jovanović *et al.* of measurements for six bands of $^{12}CD^+$,[16] followed two years later by Grieman *al.*[11] measurements for higher-J transitions in two of those bands, and another two years later by their observation of the same six bands of $^{13}CH^+$.[20] A little later, however, most of their results were superseded by the much higher resolution (±0.004–0.03 cm^{-1}) data reported by Bembenek and co-workers, first for $^{12}CD^+$,[22] and a decade later also for $^{13}CH^+$,[24] and for $^{13}CD^+$,[25] and the only Antić-Jovanović *et al.* data retained in our analysis were their results for the in 3–1 band of $^{13}CH^+$,[20] which was not observed by Bembenek.[24] Note, however, that their assigned J values[22] for the $Q(6)$–$Q(8)$ and $R(6)$–$R(1)$ lines of $^{12}CD^+$ should all be increased by 1.[57]

B. Photodissociation and translational spectroscopy data

The horizontal line segments in Fig. 1 indicate the energies of the vibrational levels of the $X^1\Sigma^+$ and $A^1\Pi$ states of CH^+ observed by "conventional" spectroscopy. It is clear that these data do not extend far enough to allow an accurate determination of the depths and the upper portions of the potential energy wells for these states, especially for the case of the ground $X^1\Sigma^+$ state. Fortunately, in the early 1980's a new experimental method was developed for the study of molecular ions, in which the observable was not the emission or absorption of light but rather the fragmentation of the molecular ion and the appearance of "daughter" ions. The measurable properties in this experiment were the photon energies that created the daughter ions, and sometimes also the relative kinetic energy of the fragments. The first application of this technique to CH^+ was the work of Cosby *et al.*[17] who observed C^+ ion production on excitation of CH^+ at 37 discrete energies within 350 cm^{-1} of the $A(^1\Pi)$-state dissociation threshold.

Two years later Helm *et al.*[18] extended those results and reported a remarkable analysis that definitively assigned the predissociating species as very high-J' ($J' = 12$–35) tunneling-predissociation levels (shape resonances) of vibrational levels $v' = 0$–10 of the $A(^1\Pi)$-state, for more than half of which they were also able to measure the photofragment kinetic energy release. Fig. 2 illustrates the nature of this predissociation process for the case of a centrifugal potential associated with $J = 32$. For this particular case, the tunneling lifetime of level $v_A = 0$ (at 877 yr) would be far too long for its fragmentation to be observed, but those for the $v_A = 1$ and 2 levels placed them within the observation

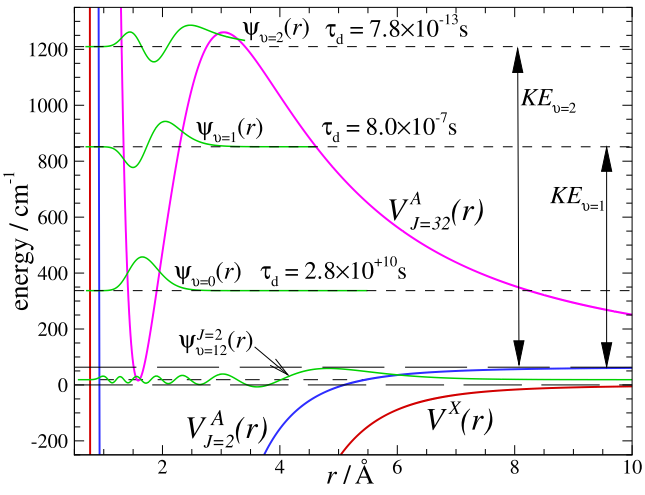

FIG. 2. Energies and wavefunctions of the $v = 0$–2 A-state quasibound or tunneling-predissociation levels (shape resonance) for $J = 32$ observed and assigned by Helm *et al.*,[18] who also reported photo-fragment kinetic energies (KE_v) for some levels. The centrifugally distorted $V^A_{J=32}$ potential is shown as a purple curve, while the blue curve going to the upper asymptote is the $V^A_{J=2}$ potential supporting the $v_A = 12$ Feshbach predissociating level whose wavefunction is shown near the bottom of this figure. The horizontal long-dash lines represent the asymptotes of the A and X state potentials that are separated by the $2P_{3/2} - 2P_{1/2}$ spin-orbit splitting of the C^+ ion, $\delta E = 63.395$ cm^{-1}, while the red curve is the potential function of the $X^1\Sigma^+$ state.

This article is copyrighted as indicated in the article. Reuse of AIP content is subject to the terms at: http://scitation.aip.org/termsconditions. Downloaded to IP: 129.97.80.15 On: Wed, 13 Jan 2016 18:34:46

window. The assignment of these data would have been greatly facilitated by the fact that the spectroscopic properties of the lower vibrational levels of both the $A^1\Pi$ and $X^1\Sigma^+$ states were known from conventional spectroscopy. However, experimental difficulties meant that the uncertainty associated with the determination of $X \rightarrow A$ line positions (~2 cm^{-1}) was relatively large, and those associated with measurement of the relative fragment kinetic energies (20–152 cm^{-1}) were even larger.[58] A few years later, a few of these high-J shape resonance transitions with predissociative linewidths of ~5 cm^{-1} remeasured by Sarre *et al.*,[23] for whose positions we have also assigned uncertainties of ±2.0 cm^{-1}, although one obvious outlier was excluded from the analysis.

Another novel experiment was reported by Hechtfischer *et al.*[26] who used photodissociation spectroscopy to observe transitions to $A(^1\Pi)$-state "Feshbach resonance" levels at low J and very high $v'(A) = 11$–14 and obtained the first direct estimate of the $^{12}CH^+$ dissociation energy with near-spectroscopic accuracy (±1.1 cm^{-1}). The wavefunction of one of these predissociating levels is shown near the bottom of Fig. 2, lying in the interval between the X and A state asymptotes, where it mixes with continuum wavefunctions associated with the $X(^1\Sigma^+)$ state, while Fig. 3 shows this region on an expanded scale. The difference between the $A(^1\Pi)$ and $X(^1\Sigma^+)$-state asymptotes is the C^+ fragment energy splitting into the $^2P_{1/2} - {}^2P_{3/2}$ fine-structure states that are separated by 63.395 cm^{-1}.[59] The $v(A) = 11$ level lies below the X-state asymptote for $J = 2$ and hence is not in the observation window of Fig. 3. We used the reported linewidths as our estimated uncertainties for the energies of these transitions.

Finally, in view of the impressive sophistication and thoroughness of the photodissociation spectra modelling and fitting reported by Hechtfischer *et al.*,[26] we introduced their recommended ground-state dissociation energy $\mathfrak{D}_0(X) = 32\,946.7(\pm 1.1)\,\text{cm}^{-1}$ as a photoassociation-like ground-state binding energy datum in our analysis. However, when at the end this datum was removed temporarily, it changed our fitted well depth by far less than the parameter uncertainties (see Section V).

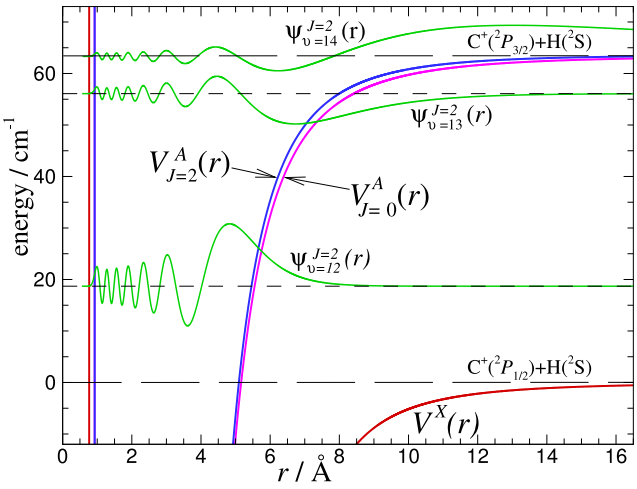

FIG. 3. Energies, wavefunctions, and supporting potentials for Feshbach resonance levels $v_A = 12$–14 for $J = 2$, observed by Hechtfischer *et al.*[26] The red curve is the $X^1\Sigma^+$ state potential, the purple curve is $A^1\Pi$ state potential for $J = 0$, and blue curve is the $A^1\Pi$ state potential for $J = 2$. The black long-dash lines indicate the dissociation limits of the A and X states.

III. METHODOLOGY

Following the approach of recent work in our group,[53,60–63] the present study is a DPF analysis in which exact quantum mechanical calculations generate predicted spectral properties from some chosen model potential energy, BOB, and Λ-doubling functions, and a least-squares fitting procedure optimizes the values of the parameters defining those functions. As in that work, the upper and lower levels defining the observed transitions are eigenvalues of the effective radial Schrödinger equation[53,64,65]

$$\left\{-\frac{\hbar^2}{2\mu_\alpha}\frac{d^2}{dr^2} + \left[V_{\rm ad}^{(1)}(r) + \Delta V_{\rm ad}^{(\alpha)}(r)\right] + \frac{[J(J+1)-\Lambda^2]\hbar^2}{2\mu_\alpha r^2}\left[1 + g^{(\alpha)}(r)\right]\right\}\psi_{v,J}(r) = E_{v,J}^{(\alpha)}\,\psi_{v,J}(r), \quad (1)$$

in which "α" labels a particular isotopologue and $\alpha = 1$ a chosen reference isotopologue, $V_{\rm ad}^{(\alpha=1)}(r)$ is the analytic potential energy function being fitted, and the potential-energy and centrifugal BOB functions, $\Delta V_{\rm ad}^{(\alpha)}(r)$ and $g^{(\alpha)}(r)$, respectively, are written as mass-weighted sums of terms associated with the two atoms,[64,66,67]

$$\Delta V_{\rm ad}^{(\alpha)}(r) = \frac{\Delta M_{\rm A}^{(\alpha)}}{M_{\rm A}^{(\alpha)}}\,\widetilde{S}_{\rm ad}^{\rm A}(r) + \frac{\Delta M_{\rm B}^{(\alpha)}}{M_{\rm B}^{(\alpha)}}\,\widetilde{S}_{\rm ad}^{\rm B}(r). \quad (2)$$

$$g^{(\alpha)}(r) = \frac{M_{\rm A}^{(1)}}{M_{\rm A}^{(\alpha)}}\,\widetilde{R}_{\rm na}^{\rm A}(r) + \frac{M_{\rm B}^{(1)}}{M_{\rm B}^{(\alpha)}}\,\widetilde{R}_{\rm na}^{\rm B}(r), \quad (3)$$

in which $\Delta M_{\rm A/B}^{(\alpha)} \equiv M_{\rm A/B}^{(\alpha)} - M_{\rm A/B}^{(1)}$ is the difference between the masses of atom A or B in isotopologue-α and in the reference isotopologue. For a molecular ion such as CH^+, the value of the effective reduced mass for a species with overall charge "Q" comprised of atoms of mass $M_{\rm A}$ and $M_{\rm B}$, is conventionally represented by[66]

$$\mu_\alpha \equiv \frac{M_A\,M_B}{M_A + M_B - {\rm Q}\times {\rm m_e}}, \quad (4)$$

in which m_e the electron mass. However, other choices for the definition of the reduced mass are also considered, and a different one is adopted for defining our final results (see Section V).

Since the A state has $^1\Pi$ symmetry, the non-zero value of its electronic angular momentum ($\Lambda = 1$) is taken into account in the centrifugal potential in Eq. (1). The associated Λ-doubling is then taken into account by including the following function as an additional potential energy term

This article is copyrighted as indicated in the article. Reuse of AIP content is subject to the terms at: http://scitation.aip.org/termsconditions. Downloaded to IP: 129.97.80.15 On: Wed, 13 Jan 2016 18:34:46

on the left-hand-side of Eq. (1),[68]

$$\mathrm{sg}_{\mathcal{A}}(e/f)\,\Delta V_{\Lambda}(r)[J(J+1)]^{\Lambda} = \mathrm{sg}_{\mathcal{A}}(e/f)\left\{\left(\frac{\hbar^2}{2\mu_\alpha\, r^2}\right)^{2\Lambda} f_{\Lambda}(r)\right\}[J(J+1)]^{\Lambda}, \quad (5)$$

in which we set (in the present case) $\mathrm{sg}_{\mathcal{A}}(e/f) = +1$, and 0 for e and f levels, respectively,[68] since it can reasonably be assumed that the state, coupling to which gives rise to this splitting, is the ground $X^1\Sigma^+$ state. The Λ-doubling radial strength function $f_{\Lambda}(r)$ is then written as a simple polynomial of order N_{Λ} in the radial variable

$$y_{p_{\Lambda}}^{\mathrm{eq}}(r) = \frac{r^{p_{\Lambda}} - {r_e}^{p_{\Lambda}}}{r^{p_{\Lambda}} + {r_e}^{p_{\Lambda}}}. \quad (6)$$

The conventional "band constant" Λ-doubling parameters q_v are, of course, the radial expectation values of the function $\Delta V_{\Lambda}(r)$ for the various vibrational levels v.

In the present work, the reference-isotopologue potential energy functions for both electronic states are represented by the later version[69–71] of the Morse/Long-Range (MLR) function[72–74]

$$V_{\mathrm{MLR}}(r) = \mathfrak{D}_e\left(1 - \frac{u_{\mathrm{LR}}(r)}{u_{\mathrm{LR}}(r_e)}\, e^{-\beta_{\mathrm{MLR}}(r)\cdot y_p^{\mathrm{eq}}(r)}\right)^2, \quad (7)$$

in which $\mathfrak{D}_e$ and r_e are the well depth and the location of the potential minimum, while the limiting long-range behaviour is defined by the long-range tail function $u_{\mathrm{LR}}(r)$, and the exponent coefficient $\beta(r)$ is a slowly varying function of r whose limiting long-range value of

$$\beta_{\infty} \equiv \lim_{r\to\infty}\beta(r) = \ln\left\{\frac{2\,\mathfrak{D}_e}{u_{\mathrm{LR}}(r_e)}\right\} \quad (8)$$

means that the limiting long-range behaviour of the potential is

$$V_{\mathrm{MLR}}(r) \simeq \mathfrak{D}_e - u_{\mathrm{LR}}(r) + \frac{\{u_{\mathrm{LR}}(r)\}^2}{4\mathfrak{D}_e} - \cdots. \quad (9)$$

The radial variable $y_p^{\mathrm{eq}}(r)$ in the exponent of Eq. (7) has the same form as Eq. (6), but is defined by a different integer p (see below).

The long-range tail function in Eq. (7) is written as a finite sum of inverse-power terms that may include "damping functions" $D_m(r)$[71]

$$u_{\mathrm{LR}}(r) = D_{m_1}(r)\,\frac{C_{m_1}}{r^{m_1}} + D_{m_2}(r)\,\frac{C_{m_2}}{r^{m_2}} + \cdots + D_{m_{\mathrm{last}}}(r)\,\frac{C_{m_{\mathrm{last}}}}{r^{m_{\mathrm{last}}}}. \quad (10)$$

The set of inverse powers appearing in Eq. (10) is determined by the nature of the atomic species into which the particular molecular state dissociates, while the C_{m_i} coefficients are (usually) determined by theory. In the present case, we retained the three longest-range terms in this sum, which for a molecular ion are $m = 4$, 6, and 8. Our value of leading inverse-power coefficient, C_4, is taken from a very recent calculation of the H atom polarizability by Lach and Dattani,[75] while the C_6 values were the theoretical estimate reported by Hechtfischer *et al.*[26] In our preliminary work, our C_8 values were fixed at the empirical values of Hechtfischer *et al.*,[26] but when they were later treated as additional free parameters (as they were in Ref. 26), our new fitted values differed from theirs by less than the associated uncertainties, so the original C_8 values of Hechtfischer *et al.*[26] were used in our final fits. As in other recent work,[60,62,63,71,76] the damping functions were represented by the "$s = -1$" version of the modified Douketis-Scoles function of Ref. 71, with the system-dependent distance scaling parameter set (following their approach) at $\rho = 1.19$.

Finally, the exponent coefficient function

$$\beta(r) = \beta_{p,q}^{\mathrm{ref}}(r) = y_p^{\mathrm{ref}}(r)\,\beta_{\infty} + \left[1 - y_p^{\mathrm{ref}}(r)\right]\sum_{i=0}^{N_\beta}\beta_i\, y_q^{\mathrm{ref}}(r)^i \quad (11)$$

is expanded as a function of two dimensionless radial variables

$$y_p^{\mathrm{ref}}(r) = \frac{r^p - {r_{\mathrm{ref}}}^p}{r^p + {r_{\mathrm{ref}}}^p} \quad \text{and} \quad y_q^{\mathrm{ref}}(r) = \frac{r^q - {r_{\mathrm{ref}}}^q}{r^q + {r_{\mathrm{ref}}}^q}, \quad (12)$$

which have the same form as Eq. (6) but are both centred at a common manually optimized distance "r_{ref}" that lies between the equilibrium distance r_e and the outer end of the data-sensitive region (defined by the inner and outer turning points of the highest observed vibrational level). There are no formal constraints on the power q defining the dimensionless expansion variable $y_q^{\mathrm{ref}}(r)$ but to prevent the effect of the long-range tail of the exponential term in Eq. (7) from changing the effective values of the chosen C_m long-range coefficients, the power p defining the switching-function variable $y_p^{\mathrm{ref}}(r)$ must be set larger than the difference between the highest and lowest (inverse) powers of the terms included in the Eq. (10) definition of $u_{\mathrm{LR}}(r)$.[71] In the present case that means that necessarily $p > m_{\mathrm{last}} - m_1 = 4$. Similarly, to prevent the $(C_4)^2$ factor in the quadratic term in Eq. (9) from changing the effective value of C_8 in the long = range potential,[69] the desired input value of C_8 is internally replaced by $C_8^{\mathrm{eff}} = C_8 + (C_4)^2/(4\mathfrak{D}_e)$ before calculating the potential.[53]

As in earlier work,[60–63,69] the potential-energy and centrifugal BOB radial strength functions of Eqs. (2) and (3) were represented by the type of constrained radial power series expansions first introduced in Ref. 65,

$$\widetilde{S}_{\mathrm{ad}}^{A/B}(r) = y_{p_{\mathrm{ad}}}^{\mathrm{eq}}(r)\,u_{\infty}^{A/B} + \left[1 - y_{p_{\mathrm{ad}}}^{\mathrm{eq}}(r)\right]\sum_{i=0}^{N_{\mathrm{ad}}^{A/B}} u_i^{A/B}\, y_{q_{\mathrm{ad}}}^{\mathrm{eq}}(r)^i, \quad (13)$$

and

$$\widetilde{R}_{\mathrm{na}}^{A/B}(r) = y_{p_{\mathrm{na}}}^{\mathrm{eq}}(r)\,t_{\infty}^{A/B} + \left[1 - y_{p_{\mathrm{na}}}^{\mathrm{eq}}(r)\right]\sum_{i=0}^{N_{\mathrm{na}}^{A/B}} t_i^{A/B}\, y_{q_{\mathrm{na}}}^{\mathrm{eq}}(r)^i. \quad (14)$$

All of the dimensionless radial variables in these expressions $y_{p/q}^{\mathrm{eq}}(r)$ have the form of Eq. (6) but are characterized by independent values of the integer powers p and q. Following the discussion of Ref. 65, to ensure that the long-range potentials for all isotopologues are exactly the same, the value of p_{ad} must be larger than the (inverse) power of the highest-order term included in the definition of $u_{\mathrm{LR}}(r)$: $p_{\mathrm{ad}} > m_{\mathrm{Last}}$.[77] However, there are no analogous physical constraints on the values of p_{na}, q_{ad}, or q_{na}.

The physical arguments of Ref. 65 imply that since BeH^+ is a molecular ion, the limiting asymptotic value

This article is copyrighted as indicated in the article. Reuse of AIP content is subject to the terms at: http://scitation.aip.org/termsconditions. Downloaded to IP: 129.97.80.15 On: Wed, 13 Jan 2016 18:34:46

of our $\widetilde{R}_{na}^{H/C^+}(r)$ functions for both states should be $t_\infty = m_e/m_{Be} \approx 6.1 \times 10^{-5}$. However, this value is sufficiently small relative to the radial variation of these functions that for the sake of simplicity, we fix all four t_∞ values as zero, the same value that they would have for a species that dissociates to neutral fragments.[65] Similarly, as for all species dissociating to ground-state atomic fragments, $u_\infty^{H/C^+} = 0$ for the ground state, and since the $^{12}C^+ \rightarrow {}^{13}C^+$ isotope splitting of the $C^+(^2P_{1/2} - {}^2P_{3/2})$ transition energy is extremely small (3.7×10^{-5} cm^{-1}),[59] we fix $u_\infty^{H/C^+} = 0$ for the excited state too.

IV. DPF ANALYSIS FOR THE $X^1\Sigma^+$ AND $X^1\Sigma^+$ STATES OF CH^+

A. The potential energy functions

The analysis began by determining a model potential energy function for the $X^1\Sigma^+$ state from fits that treated all relevant levels of the $A^1\Pi$-state as independent term values. As was pointed out in Refs. 71 and 73, within the MLR potential function model, the first exponent expansion-variable power "p" is required to be larger than the difference between the powers of the first and last terms in the long-range potential of Eq. (10), which for our case are $m_i = 4$, 6, and 8. Thus, a series of fits was performed for each of $p = 5$ and 6 and a range of r_{ref} values. These initial fits proved to be fairly insensitive to the location of the expansion centre r_{ref}, and it was set a value of 1.3 Å located roughly mid-way between r_e and the outer end of the data-sensitive region. Determination of the optimum value of the power N_β of the exponent-expansion polynomial was quite straightforward, since values of $N_\beta \leq 5$ gave fits of unacceptably poor quality, while for $N_\beta \geq 7$ the quality of fit improved little and one or more of the fitted exponent expansion coefficients β_i had uncertainties of 100% or more. Finally, there are no formal constraints on the value of the second exponent-expansion function power q, other than the requirement that the interpolation/extrapolation from the outer end of the "data-sensitive region" to the limiting long-range region where the potential becomes Eq. (10), must be "physically sensible," and here we have a problem.

The dashed and solid red curves on Fig. 1 show that different choices of the MLR exponent-expansion variable integers p and q give rise to widely different types of interpolation/extrapolation behaviour beyond the outer end of the data-sensitive region at about 1.54 Å, some of which is patently unphysical, with spurious extra inflection points or even an artificial second minimum. In the absence of any additional information, "*Occam's razor*" arguments would have led us to choose the $\{p = 5,\ q = 1\}$ model, shown as a solid red curve in Fig. 1, as the physically most plausible potential function that we could determine from the experimental data alone, since it seemed the farthest removed from spurious second-inflection-point behaviour seen for other cases and had the most plausible fully "concave" shape of the cases considered.

Fortunately, although there is no *experimental* information about the $X^1\Sigma^+$-state potential in the region beyond the outer turning point of vibrational level $v_X = 3$, high quality *ab initio* calculations have been reported that give us guidance (open points on Fig. 1).[23,78–80] In particular, we see that the potential function values reported by Saxon *et al.* in 1980 (round magenta points) and Sarre, Whitham, and Graff in 1989 (square purple points) are in remarkably good agreement with those calculated by Sauer and Špirko (square blue points) and Biglari *et al.* (diamond-shaped red points) some 25 years later, regarding the shape and depth of the $X^1\Sigma^+$-state potential, although the analyses of Hechtfischer *et al.*[26] and the present work (solid black curve) show that their well depths were slightly too small. Nevertheless, since the present empirical analysis needs assistance at distances beyond ~1.5 Å, we selected the two Sauer and Špirko *ab initio* potential function values identified by black circles on Fig. 1 and included them as pseudo-experimental data in our fits. Although the uncertainties of 1.0 cm^{-1} assigned to these two points were quite small, the residual discrepancies found after including them in the fit were a more that an order of magnitude smaller than that. The resulting potential is the $\{p,q\} = \{5,1\}$ solid black curve in Fig. 1, and because of the high degree of inter-parameter correlation, essentially the same quality of fit to the experimental data is achieved with no increase in the number of expansion parameters or change in the form of the model. Moreover, equally good fits were also obtained using larger values of q. However, as might be expected, inclusion of these larger-r potential function points as data meant that the optimum value of the expansion centre r_{ref} became somewhat larger. It is also interesting to note that this constraint imposing physically correct behaviour on the attractive outer wall induced the extrapolated short-range repulsive wall of the resulting fitted $\{p = 5,\ q = 1\}$ potential (solid black curve) to be in much closer agreement with the *ab initio* points in the inner-wall region.

A final test was to examine whether our optimum fitted potential behaves well in the extrapolation region between the outer turning point of the highest observed level and the asymptotic limit where $r \rightarrow \infty$.[53,63] Since our long-range potential consists of three inverse-power terms with $m_i = 4$, 6, and 8, Eqs. (9) and (10) suggest that a plot of $C_4^{eff}(r) \equiv r^4[\mathfrak{D} - V(r)]$ *vs.* $1/r^2$ should approach an $r \rightarrow \infty$ intercept of C_4^{theory} with a limiting slope of C_6^{theory}. Fig. 4 shows the behaviour of a few different MLR models in this extrapolation region. All curves *must* (by construction) approach the correct C_4^{theory} intercept with the correct (very small) limiting slope of C_6^{theory}, and this is clearly the case. Moreover, since the C_8/r^8 term is attractive, we expect these plots to approach this limiting slope from above, and this is clearly also true for most of these functions. However, for most of the models illustrated here there is an implausible "bulge" in the extrapolated curve near $1/r^2 = 0.04$ (≈5 Å). In contrast, the extrapolated "$6_{5,1}$" curve behaves much more sensibly, except for a very slight dip below the predicted limiting slope, centred near an ordinate value of $1/r^2 \approx 0.007$ (≈12 Å, see Fig. 4 inset). This unphysical "dip" could be removed by tinkering with the choice (or adding to the set) of *ab initio* points being fitted to as "data." However, the resulting improvements in the potential function in this region would be less than 0.03 cm^{-1}, which is far smaller than the uncertainties in the *ab initio* points there, so we chose this "$6_{5,1}$" MLR function with $r_{ref} = 2.55$ Å as our recommended model for the ground $X^1\Sigma^+$ state of CH^+.

This article is copyrighted as indicated in the article. Reuse of AIP content is subject to the terms at: http://scitation.aip.org/termsconditions. Downloaded to IP: 129.97.80.15 On: Wed, 13 Jan 2016 18:34:46

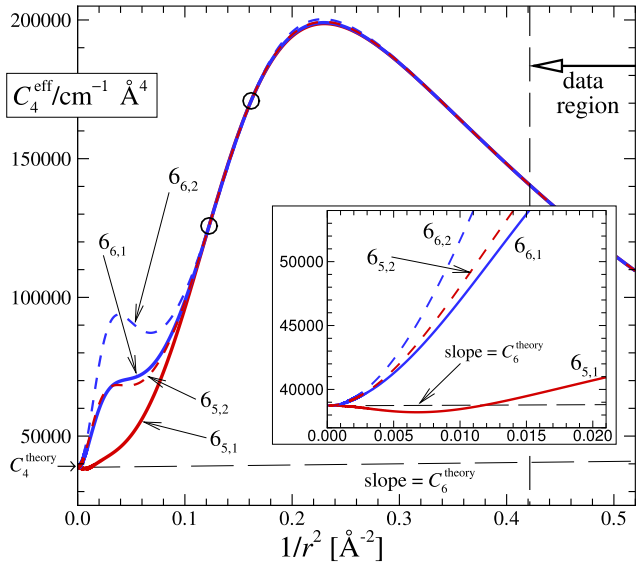

FIG. 4. $C_4^{\rm eff}$ plot showing the long-range extrapolation behaviour of various fitted MLR potential functions, $N_{p,q}$, where $N \equiv N_\beta$ is the exponent polynomial order. Curves for "$r_{\rm ref}$-optimized" $p = 5$ models are red and those for $p = 6$ models are blue, while curves for $q = 1$ models are shown as solid lines and those for $q = 2$ models as dashed ones.

Once an optimum model was determined for the $X^1\Sigma^+$ state, fits to determine one for the $A^1\Pi$-state potential were performed with the model for the $X^1\Sigma^+$-state potential held fixed, although all of its parameters were allowed to vary. Because the difference between the X- and A-state asymptotes is the accurately known $^2P_{3/2} - {}^2P_{1/2}$ excitation energy of the C^+ ion,[59] the high-v A-state data effectively determine our new improved estimate of the ground-state well depth. Once again, a MLR functional form was used, with its three leading long-range coefficients all initially held fixed, C_4 at the value defined by the very recent H atom polarizability calculation of Lach and Dattani,[75] and C_6 and C_8 at the values reported by Hechtfischer *et al.*[26] As was the case for the $X^1\Sigma^+$ state, the quality of fit depended only weakly on the value of the radial-variable expansion centre $r_{\rm ref}$ across the range considered, (2.7–4.0 Å), and we settled on the value $r_{\rm ref} = 2.96$ Å. It also quickly became clear that the optimum exponent-expansion power was $N_\beta = 8$, since smaller values gave a much lower quality of fit, while although the quality-of-fit for those with $N_\beta \geq 9$ was marginally better, one or more of the resulting β_i exponent expansion coefficients had uncertainties of >100%, and some of the resulting potentials did not support all of the observed vibrational levels. The results were also not very sensitive to the choice of the exponent-variable powers, and we chose the model with $p = 6$ and $q = 1$ as our recommended potential energy function for the $A^1\Pi$ state of CH^+.

As is shown in Fig. 1, the "conventional" data for the $A^1\Pi$ state ($v_A = 0$–4) span about half of its well,[12,13,19] and the Feshbach-resonance photodissociation study of $v_A = 11 = 14$ follows its vibrational levels virtually all the way to its asymptote,[26] so the interpolation/extrapolation problems encountered for the $X^1\Sigma^+$ state do not arise, and the analog of Fig. 4 shows sensible extrapolation behaviour for all of the models considered.

As was discussed in Section III, the Λ-doubling splitting in the $A^1\Pi$ state is accounted for by including the centrifugal-type potential term of Eq. (5) in the radial Schrödinger equation. The present analysis found that these splittings are fully accounted for when the Λ-doubling radial strength function is represented by a polynomial of order $N_\Lambda = 4$ in the radial variable $y_{p_\Lambda}^{\rm eq}$ of Eq. (6), with $p_\Lambda = 4$. The values of these expansion coefficients are listed in Table II, and a complete listing of the corresponding values of the "conventional" band

TABLE II. Parameters defining the recommended MLR potential functions for the $X^1\Sigma^+$ and $A^1\Pi$ states of CH^+, and the associated BOB and Λ-doubling radial strength functions. These parameters were obtained using conventional 2-body reduced masses for neutral C with H or D, and the reference isotopologue was $^{12}CH^+$. Numbers in parentheses are the averaged-over-models uncertainties in the last digits shown for parameters with direct physical significance.

	$X^1\Sigma^+$	$A^1\Pi$
T_e	...	24 122.496 (94)
$\mathfrak{D}_e$	34 362.8 (3)	10 303.7 (3)
r_e	1.128 462 5 (58)	1.235 896 (14)
$\rho_{\rm AB}$	1.19	1.19
$C_4/10^4$	3.878 472 36	3.878 472 36
$C_6/10^6$	0.004 3	0.107
$C_8/10^8$	1.6	3.3
$\{p, q\}$	{5, 1}	{6, 1}
$r_{\rm ref}$	2.55	2.96
β_0	−0.150 240 186	−0.726 448 35
β_1	13.729 778 8	19.172 913
β_2	71.225 228	111.206 63
β_3	213.323 2	390.443 7
β_4	380.73	1 004.442
β_5	375.29	2 075.55
β_6	157.9	3 172.0
β_7	...	2 926.7
β_8	...	1 167.0
$\{p_{\rm ad}, q_{\rm ad}\}$	{9, 1}	{9, 1}
u_0^C	[0.0]	−0.201 (78)
u_1^C	77.59	48.3
u_2^C	517.0	142.0
u_3^C	17 000.0	...
u_0^H	[0.0]	11.989 (157)
u_1^H	228.8	437.9
u_2^H	1 704.8	2 470.4
u_3^H	37 230.0	41 290.0
u_4^H	96 000.0	34 400.0
u_5^H	229 000.0	571 000.0
u_6^H	5 590 000.0	2 800 000.0
$p_{\rm na}, q_{\rm na}$	{7, 7}	{4, 4}
t_0^H	−0.004 17	[0.0]
t_1^H	−0.002 613	−0.000 056
t_2^H	...	0.017 27
q_Λ	...	{1}
ω_0	...	0.000 291 13
ω_1	...	0.000 544
ω_2	...	0.002 402
ω_3	...	−0.009 4
ω_4	...	0.079

This article is copyrighted as indicated in the article. Reuse of AIP content is subject to the terms at: http://scitation.aip.org/termsconditions. Downloaded to IP: 129.97.80.15 On: Wed, 13 Jan 2016 18:34:46

constant Λ-doubling parameters q_v are listed, together with the "mechanical" inertial rotation and centrifugal distortion constants defined by the present recommended potential energy functions, in the supplementary material.[81]

B. The Born-Oppenheimer breakdown correction functions

The potential-energy BOB correction functions $\Delta V_{\rm ad}^{(\alpha)}(r)$ define the differences between the effective adiabatic potentials for the different isotopologues, α. Following the standard convention of defining the absolute zero of energy as the energy of separated ground-state atoms or ions at rest, the limiting long-range values of the adiabatic radial strength function $\widetilde{S}_{\rm ad}^{\rm H/C}(r)$ for the $X^1\Sigma^+$ state are $u_\infty^{\rm H} = u_\infty^{\rm C} = 0$ and for the reasons given at the end of Section III, we assumed the same for the $A^1\Pi$ state. As a result, for the $X^1\Sigma^+$ state the leading polynomial coefficient in Eq. (13), u_0, defines the isotopologue dependence of its well depth, while for the $A^1\Pi$ state it defines the electronic isotope shift.[65] Unfortunately, the modest vibrational range of the available data for the $X^1\Sigma^+$ state makes it unrealistic to expect the present analysis to be able to determine the former, so our fits were performed with $u_0^{\rm H} = u_0^{\rm C} = 0.0$.

In order to ensure that the effective adiabatic minor-isotopologue potentials have exactly the same long-range tails as those for the reference isotopologues, we fixed $p_{\rm ad} = 9$,[77] and as there are no constraints on the value of $q_{\rm ad}$, we set it at the same value found to be convenient for the exponent coefficient function $q_{\rm ad} = q = 1$. Varying the value of this parameter had no significant effect on the shape of the "adiabatic" BOB functions $\widetilde{S}_{\rm ad}^{\rm C/H}(r)$ within the data-sensitive region.

Fully accommodating the data for the various carbon isotopologues required three fitted $u_i^{\rm C}$ expansion parameters for each state. As expected, the hydride isotope effects are much larger than those for the carbon ion, and our analysis required six fitted $u_i^{\rm H}$ shape parameters for the $X^1\Sigma^+$ state and seven for $A^1\Pi$. The resulting $u_0^{\rm H}$ value for the $A^1\Pi$ state indicates that its T_e value is 5.99(±0.08) cm^{-1} smaller for the deuterides than for hydride species. The analogous differences are, of course, much smaller for the carbon isotopologues, but they are still discernable, with the T_e values for ^{13}C and ^{14}C being, respectively, 0.015(±0.006) and 0.029(±0.011) cm^{-1} larger than those for the analogous ^{12}C species.

Regarding the "non-adiabatic" centrifugal BOB correction, the present analysis found that with the limits $t_0^{\rm H}$ and $t_\infty^{\rm H}$ held fixed, the fits required one empirical $t_i^{\rm H}$ parameter for the $X^1\Sigma^+$ state and two for the $A^1\Pi$ state to obtain an optimal description of the data, while if there were no empirical $t_i^{\rm H}$ parameters, the value of the "dimensionless root mean square deviation" $\overline{dd}$, our quality of fit parameter,[53,62] doubled. In contrast, no empirical $t_0^{\rm C}$ parameters could be discerned for either states.

Watson showed long ago[66,67] that while its radial dependence might be determined from this type of analysis, the absolute magnitude of the centrifugal BOB correction in Eq. (1) cannot be determined from transition-energy data alone. For such cases, he proposed the convention of requiring the value of $g^{(\alpha)}(r)$ to be zero at the equilibrium distance for that state, r_e. Within the present formulation, this means requiring the lead expansion parameter of Eq. (14), t_0, be fixed at zero, and this is what was done in our initial analyses. However, we later became aware of Amano's determination of the "rotational g-factor" for ground-state CH^+,[32] which is directly related to the expectation value of $g_{(\alpha)}(r)$ for that level. Since our analysis found no sensitivity to the $\widetilde{R}_{\rm na}^{\rm C}(r)$ function parameters, we attribute this quantity to the H-atom component $\widetilde{R}_{\rm na}^{\rm H}(r)$ and multiply the experimental g-factor by the scaling factor, $m_e/m_{\rm H}$ to obtain an estimate of $t_0^{\rm H} = -0.004\,17(16)$ for this state. Fixing $t_0^{\rm H}$ at this value rather than zero yielded a modest and probably physically significant 0.9% improvement in the quality of fit to the experimental data, and fits to the data with $t_0^{\rm H}$ fixed at this value while using four different choices for the expansion-variable parameters $p_{\rm na} = q_{\rm na}$ yielded the $\widetilde{R}^{\rm H}(r)$ functions shown as dashed and solid (the recommended model) red curves on Fig. 5. The green dashed-dotted curve shown there is the $\widetilde{R}^{\rm H}(r)$ function obtained from an analogous fit that imposed the "default" Watson constraint of fixing $t_0^{\rm H} = 0$, while the blue dashed-dotted-dotted curve with the much larger uncertainties shows the results of performing a fit with $t_0^{\rm H}$ treated as a free fitting parameter. The error bars indicating the uncertainties on the functions shown as red curves can only barely be resolved on the expanded-scale inset. Finally, the solid black points and thin black curve are the results of a recent *ab initio* calculation of this function by Sauer and Špirko.[79]

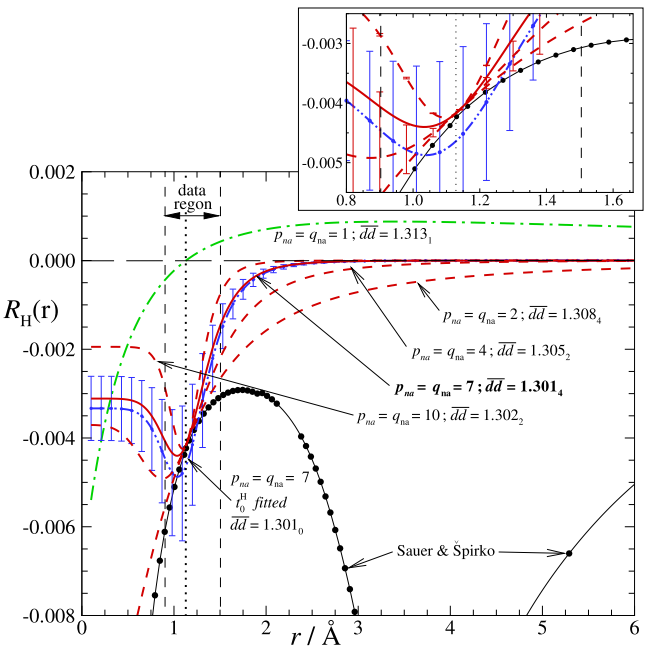

FIG. 5. Plots of the centrifugal BOB function $\widetilde{R}^{\rm H}(r)$. The black points and curve are the *ab initio* results of Sauer and Špirko,[79] the green dashed-dotted curve is the function obtained using Watson's "transition-frequency-alone" ansatz of fixing $t_0 = 0$, while the dashed and solid (recommended) red curves were obtained using $N_{\rm na} = 1$ with t_0 defined by Amano's experimental $q_{v=0}$ value[32] and various choices for $p_{\rm na} = q_{\rm na}$. Setting t_0 free yielded the blue dashed-dotted-dotted curve with its relatively large uncertainties while the analogous predicted uncertainties associated with the red and green curves are too small to be resolved except, possibly in the expanded-scale upper panel.

This article is copyrighted as indicated in the article. Reuse of AIP content is subject to the terms at: http://scitation.aip.org/termsconditions. Downloaded to IP: 129.97.80.15 On: Wed, 13 Jan 2016 18:34:46

TABLE III. Quality of fit to multi-isotopologue data for CH^+ using five definitions for the reduced masses. Values are listed in increasing order with the last column showing the % deviation from the value in the first row.

Reduced masses of	$\overline{dd}$	% difference
Neutral C and H/D atoms	1.301 42	0.000
C^+ ion with H/D atom	1.301 44	0.002
$C^{+1/2}$ ion with $H^{+1/2}$ or $D^{+1/2}$ ion	1.303 56	0.164
Watson definition of Eq. (4)	1.305 21	0.291
C atom with H^+ or D^+ ion	1.305 87	0.342

Although the differences among various cases are typically less than 1%, our quality-of-fit parameter $\overline{dd}$ does show a preference for the case with $p_{\rm na} = q_{\rm na} = 7$ for the $X^1\Sigma^+$ state and $p_{\rm na} = q_{\rm na} = 4$ for the $A^1\Pi$ state, so this is chosen as our recommended model. It is reassuring to see the good agreement of the slope of our red fitted $\widetilde{R}^{\rm H}_{\rm na}(r)$ functions in the middle of the data-sensitive region with that of the *ab initio* results of Sauer and Špirko, although the marked deviation of the latter in the outer part of the data region, and its strange oscillatory behaviour at larger r where the interaction potential is essential zero are somewhat puzzling. The very large error bars on the blue curve that was obtained with $t_0^{\rm H}$ as a free parameter, and the fact that most of the adiabatic correction parameters $u_i^{\rm H}$ yielded by that fit had >100% uncertainties provide instructive confirmation of the validity of Watson's assertion[66,67] that the absolute magnitude of the $g^{(\alpha)}(r)$ function cannot be determined from transition energy data alone and that t_0 was almost 100% correlated with u_1.

As expected, the model that used the conventional "default" assumption that $t_0^{\rm H} = 0$ (green dashed-dotted curve) that has been used in most empirical analyses that reported fitted $g^{(\alpha)}(r)$ functions in recent years,[41,60,62,63,65,69,82–90] also has a near-optimum $\overline{dd}$ value, although the resulting function is very different than the others. This underlines the point that when no magnetic splitting data are available to define the value of $q_{v=0} \approx g(r = r_e)$, the physical significance of empirical $\widetilde{R}(r)$ functions that may be required to fully explain the data may be somewhat limited. Moreover, the rather different functional behaviours of the dashed and solid red curves, even within what is normally thought of as the data-sensitive region, raises questions about the physical

TABLE IV. Comparison of some reported properties of the $A^1\Pi$ and $X^1\Sigma^+$ states of CH^+. Values in square brackets were fixed based on earlier work, those in curly brackets {...} are our estimates, based on the reported parameter set, while those in round brackets are, as usual, the estimated uncertainties in the last digits shown.

Source	$\mathfrak{D}_0/\text{cm}^{-1}$	$\mathfrak{D}_e/\text{cm}^{-1}$	r_e/Å	Method
$X^1\Sigma^+$ state				
Present work	32 946.7 (3)	34 362.8 (3)	1.128 462 5 (58)	*Empirical*
Müller[52]			1.130 848 (8)	*Empirical*
Hechtfischer[26]	32 946.7 (11)			*Expt.*
Hakalla[29]	...	38 470.0 (3503)	1.130 884 3 (30)	*Expt.*
Sarre[23]	...	[34 323.8]	[1.131]	*Empirical*
Helm[18]	32 907 (23)	{34 324 (23)}	[1.130 9]	*Expt.*
Graff[98]	...	34 364	[1.131]	*Empirical*
Grieman[11]	...	...	1.125 (4)	*Expt.*
Huber[99]	32 948 (180)	{34 301}	[1.130 9]	*Expt.*
Douglas[13]	...	...	1.130 9	*Expt.*
Douglas[12]	29 100 (1800)	...	1.131 0	*Expt.*
Biglari[80]	{32 810}	34 227	1.130	*Theory*
Sauer[79]	...	34 096.23	1.127 805	*Theory*
Barinovs[100]	32 892.51	34 393	1.127 8	*Theory*
Kanzler[101]	{36 390}	37 600	1.125	*Theory*
Saxon[78]	...	33 390	1.128 7	*Theory*
Green[102]	...	33 150	1.130 3	*Theory*
$A^1\Pi$ state				
Present work	9 401.78 (30)	10 303.7 (3)	1.235 896 (14)	*Empirical*
Müller[52]			1.234 994 (10)	*Empirical*
Hakalla[29]	...	14 415 (3509)	1.235 053 (48)	*Expt.*
Sarre[23]	...	[10 263.4]	[1.234]	*Empirical*
Helm[18]	9 351 (23)	{10 266 (23)}	[1.234 5]	*Expt.*
Graff[98]	...	10 306	[1.234]	*Empirical*
Grieman[11]	...	...	1.228 (5)	*Expt.*
Douglas[13]	...	...	1.234 5	*Expt.*
Douglas[12]	5 500 (1800)	...	1.234 5	*Expt.*
Biglari[80]	{9 108}	9 992	1.239	*Theory*
Barinovs[100]	9 304.6	10 264	1.234 0	*Theory*
Kanzler[101]	{11 311}	12 300	1.205	*Theory*
Saxon[78]	...	7 550	1.260	*Theory*
Green[102]	...	8 240	1.181	*Theory*

This article is copyrighted as indicated in the article. Reuse of AIP content is subject to the terms at: http://scitation.aip.org/termsconditions. Downloaded to IP: 129.97.80.15 On: Wed, 13 Jan 2016 18:34:46

significance of our final $\widetilde{R}^{H}(r)$ function, even though its inclusion is essential for providing an accurate representation of the experimental data.

V. DISCUSSION AND CONCLUSIONS

In their landmark DPF study of the HeH^+ system, Coxon and Hajigeorgiou[84] discussed the effect of using different choices for the definition of the reduced masses of the diatomic ions on the overall quality-of-fit in their four-isotopologue analysis. In particular, although no quantitative measure was provided, they reported that use of the charge-adjusted mass of Eq. (4) yielded a significantly better fit than did use of conventional 2-body reduced masses for the bare nuclei or (by implication) of the natural dissociation products, He with H^+ or D^+, but that their best fit was obtained using 2-body reduced masses for $He^{+1/2}$ with $H^{+1/2}$ or $D^{+1/2}$. We therefore compared three of these cases together with two others: assigning all of the lost electron mass to the atom with the *higher* ionization energy (H or D in our case), and using simple 2-body reduced masses of the atomic components with *no* adjustments for loss of electron mass. Table III compares the results of this study. It clearly shows that assigning half of the lost electron mass to each fragment (row 3) is again better than use of the charge-adjusted masses of Eq. (4) (row 4) but that the best fits were obtained using 2-body masses for the actual dissociation products, C^+ with H or D (row 2), and (perhaps surprisingly) the 2-body masses for the neutral atoms (row 1). While the two best cases give fits of essentially equal quality, because it would probably be simpler for most users, the final recommended parameter set of Table II was based on fits using the 2-body neutral-atom reduced masses of the C and H or D atom pairs. Hence, these are the reduced masses that should be used in calculations utilizing these potentials. However, while the results presented in Table III are very intriguing, it would be premature to attempt to draw any general conclusions based on results for a single system. This question will be re-examined on completion of our analogous studies of HeH^+ and BeH^+.[91,92]

In summary, the present analysis has been able to combine all of the available "conventional" spectroscopic data for four isotopologues of CH^+ with two types of photodissociation data (transition energies and fragment kinetic energies) from multiple sources, plus two *ab initio* points, in a unified analysis that yields analytic potential energy functions, and BOB and Λ-doubling radial strength functions for the $X^1\Sigma^+$ and $A^1\Pi$ states of isotopic CH^+ that can account for all of the data (on average) within their uncertainties and can provide realistic predictions for all of the predicted 25 vibrational levels of ground-state CH^+, 34 of CD^+, and 40 of CT^+. We believe that the fact that our final $\overline{dd} = 1.303$ is slightly larger that unity probably merely reflects the difficulty of estimating the uncertainties associated with the photodissociation data, and undue optimism in the reported estimates for some of the other data uncertainties.[93]

The results of this analysis are summarized in Table II. While the conventional data for the $X^1\Sigma^+$ state of CH^+ only involved levels lying far below the dissociation limit (up to $v'' = 3$), the $A^1\Pi$ state is essentially fully defined due to the combination of conventional transition energy data and very high-J tunneling predissociation data for the lower levels with low-J Feshbach resonance photodissociation data for the highest levels, and the detailed simulation analysis of Hechtfischer *et al.*[26] yielded a value of $\mathfrak{D}_0(X) = 32\,946.7 \pm 1.1\ cm^{-1}$ that we used as a datum in our final analyses. The parameters listed in Table II were obtained following application of the "sequential rounding and refitting" (SRR) procedure of Ref. 94, with each rounding step being performed at the second digit of the parameter uncertainty. This leads to a optimally compact (requiring as few significant digits as possible) set of parameters with minimal (0.03% in this case) loss of precision.

It is normally the case that at least some of the parameter uncertainties associated with a fit to any particular model will be substantially smaller than the variation of the parameter values themselves from one otherwise equivalent model to another.[60,62,95] To take account of the additional uncertainties due to this "model-dependence" we have applied the "averaging-over-models" method of Ref. 95 to all of the physically significant parameters determined in our CH^+ analysis. Averaging over 25 models with different q and/or r_{ref} values whose $\overline{dd}$ values lay within 1% of the minimum, yielded the parameter uncertainties shown in parentheses in Table II. The resulting total estimated uncertainty in the ground state well depth, $\pm 0.30\ cm^{-1}$, is roughly the same as the values yielded by the individual fits, and this was also the case for the electronic isotope shift parameters $u_0^{C/H}$. However, the analogous values for the X and A state bond lengths, 5.8×10^{-6} and 5.8×10^{-6} Å, respectively, are an order of magnitude larger than those associated with the individual fits. Note that performing this averaging over the 18 models whose $\overline{dd}$ values lay within 0.5% of the minimum or the 27 models whose $\overline{dd}$ values lay within 0.5% of that minimum does not change these uncertainties significantly.

In conclusion, the $\pm 0.3\ cm^{-1}$ uncertainty in the value of $\mathfrak{D}_e$ yielded by the present fits is probably a realistic estimate of the uncertainty in the ground-state well depth, and 6×10^{-6} Å a realistic estimate of the uncertainty in our knowledge of its bond length, within the limits of our Hamiltonian, Eq. (1). In contrast, the uncertainties in our estimates of $T_e(A)$ and its isotopologue dependence are somewhat smaller, because, they depend more directly on the high resolution transition energy data used in the analysis. Note, however, that in an equivalent fit in which that Hechtfischer *et al.* $\mathfrak{D}_0$ value[26] was *not* included as a datum, the estimated parameter uncertainty for $\mathfrak{D}_e$ was the same as their $\mathfrak{D}_0$ uncertainty of $\pm 1.1\ cm^{-1}$, while the resulting estimate of $\mathfrak{D}_0$ differed from their value by less than half that amount.

Table IV compares our present estimates of the dissociation energies $\mathfrak{D}_0$, well depths $\mathfrak{D}_e$, and equilibrium distances r_e of the $X^1\Sigma^+$ and $A^1\Pi$ states of CH^+ with previous experimental and theoretical predictions. Figure 1 showed that the older *ab initio* calculation for the $A^1\Pi$ state[78] (open round points) define a potential that is distinctly shallower than that determined by the present empirical analysis (solid black curve), although their shapes are very similar, and that the very recent results of Biglari *et al.*[80] (red diamond shaped points) are much better, while for the ground state, the 2013 potential

This article is copyrighted as indicated in the article. Reuse of AIP content is subject to the terms at: http://scitation.aip.org/termsconditions. Downloaded to IP: 129.97.80.15 On: Wed, 13 Jan 2016 18:34:46

energy points of Sauer and Špirko[79] (green delta points) lie in between those two sets of results. On the scale of the Fig. 1 inset, the 1989 semi-empirical potential of Sarre[23] appears to be in excellent agreement with the present recommended potential; however, Table IV confirms that its well depth, which was based on the 1982 results of Helm *et al.*,[18] is also slightly too small. Finally, the fact that the present X-state dissociation energy $\mathfrak{D}_0$ is not significantly different from that of Hechtfischer *et al.*,[26] which is not surprising, since both critically depend upon their remarkable Feshbach predissociation measurements. However, their work did not yield an actual explicit potential energy function for either state, and the present independent-channel effective-adiabatic-potential analysis seems considerably more transparent than the coupled-channel simulations they describe.

As a final point, we draw attention to the equilibrium bond length comparisons in column 4 of Table IV, where we see that the present values differ from those yielded by the meticulous analysis of Müller,[52] which are roughly in accord with those from most earlier empirical analyses, by orders of magnitude more than the mutual uncertainties. We believe that this illustrates fundamental weaknesses of *all* traditional analyses based on fits to Dunham-type expansions that rely on extrapolation to a fictitious non-physical $v = -1/2$ point to define the potential minimum. These weaknesses are first, the dependence on a first-order semiclassical description whose accuracy is lowest for small reduced mass species such as hydrides; second, the fact that the effect of the BOB corrections that make the potential energy functions slightly different for different isotopologues cannot be distinguished from the effects of breakdown of the first-order semiclassical quantization condition; and third, this traditional one-dimensional extrapolation to $v = -1/2$ offers no natural way of testing for model-dependence. In contrast, in a DPF analysis the use of numerically exact quantum calculations to simulate the data completely removes all questions associated with semiclassical approximations, the BOB effects are explicitly delineated, and model-dependence can readily be examined.

In closing, we wish to emphasize that although inclusion of an empirical centrifugal BOB function is necessary to account optimally for the vagaries of the data, the physical significance of the resulting radial strength function may be somewhat limited.

Supplementary material associated with this work includes:[81] full lists of all the experimental data used in the analysis and of the `[calc.-obs.]` values from the final fit, tables of band constants for all vibrational levels of all isotopologues supported by our potentials, including those for the unobserved tritium species, a Fortran subroutine for generating the effective adiabatic potential of all isotopologues in both states, and sample input data files for using our potentials in the "industry standard" bound-state Franck-Condon factor program LEVEL.[96]

ACKNOWLEDGMENTS

We thank Dr. Holger Müller for providing and discussing with us the data used in his critical 2010 reassessment of CH^+ [52] and for thoughtful comments on our manuscript, and Professor Takayoshi Amano for helpful discussions, both regarding this system in general, and regarding the uncertainties associated with his very recent data for it.[33] We are also grateful to Dr. Nike Dattani for helpful discussions regarding the nature and representation of Born-Oppenheimer breakdown functions. We are also pleased to acknowledge the support of the Natural Sciences and Engineering Research Council of Canada through the award of a "Discovery Grant" to R.J.L.

[1]A. E. Douglas and G. Herzberg, Astrophys. J. **94**, 381 (1941).
[2]H. N. Russell, Mon. Not. R. Astron. Soc. **95**, 610 (1935).
[3]P. Swings, Mon. Not. R. Astron. Soc. **97**, 212 (1937).
[4]P. Swings and L. Rosenfeld, Astrophys. J. **86**, 483 (1937).
[5]S. A. S. Eddington, The Observatory **60**, 99 (1937).
[6]P. W. Merrill, Publ. Astron. Soc. Pac. **46**, 206 (1934).
[7]P. W. Merrill, Astrophys. J. **83**, 126 (1936).
[8]J. T. Dunham, Publ. Astron. Soc. Pac. **49**, 26 (1937).
[9]W. S. Adams, Astrophys. J. **93**, 11 (1941).
[10]P. M. Solomon and W. Klemperer, Astrophys. J. **178**, 389 (1972).
[11]F. J. Grieman, B. H. Mahan, A. O'Keefe, and J. S. Winn, Faraday Discuss. Chem. Soc. **71**, 191 (1981).
[12]A. E. Douglas and G. Herzberg, Can. J. Res. **20a**, 71 (1942).
[13]A. E. Douglas and J. R. Morton, Astrophys. J. **131**, 1 (1960).
[14]M. Carre, Physica **41**, 63 (1969).
[15]H. Cisak and M. Rytel, Acta Phys. Pol., A **39**, 627 (1971).
[16]A. Antić-Jovanović, V. Bojivić, D. S. Pešić, and S. Weniger, J. Mol. Spectrosc. **75**, 197 (1979).
[17]P. C. Cosby, H. Helm, and J. T. Moseley, Astrophys. J. **235**, 52 (1980).
[18]H. Helm, P. C. Cosby, M. M. Graff, and J. T. Moseley, Phys. Rev. A **25**, 304 (1982).
[19]A. Carrington and D. A. Ramsey, Phys. Scr. **25**, 272 (1982).
[20]A. Antić-Jovanović, V. Bojović, D. S. Pešić, and S. Weniger, Spectrosc. Lett. **16**, 11 (1983).
[21]A. Carrington and T. P. Softley, Chem. Phys. **206**, 315 (1986).
[22]Z. Bembenek, H. Cisak, and R. Kępa, J. Phys. B **20**, 6197 (1987).
[23]P. J. Sarre, C. J. Whitham, and M. M. Graff, J. Chem. Phys. **90**, 6061 (1989).
[24]Z. Bembenek, J. Mol. Spectrosc. **181**, 136 (1997).
[25]Z. Bembenek, J. Mol. Spectrosc. **182**, 439 (1997).
[26]U. Hechtfischer, C. J. Williams, M. Lange, J. Linkemann, D. Schwalm, R. Wester, A. Wolf, and D. Zajfman, J. Chem. Phys. **117**, 8754 (2002).
[27]E. Falgarone, T. G. Phillips, and J. C. Pearson, Astrophys. J., Lett. **634**, L149 (2005).
[28]J. C. Pearson and B. J. Drouin, Astrophys. J., Lett. **647**, L83 (2006).
[29]R. Hakalla, R. Kępa, W. Szajna, and M. Zachwieja, Eur. Phys. J. D **38**, 481 (2006).
[30]U. Hechtfischer, J. Rostas, M. Lange, J. Linkemann, D. Schwalm, R. Wester, A. Wolf, and D. Zajfman, J. Chem. Phys. **127**, 204304 (2007).
[31]T. Amano, Astrophys. J., Lett. **716**, L1 (2010).
[32]T. Amano, J. Chem. Phys. **133**, 244305 (2010).
[33]S. Yu, B. Drouin, J. Pearson, and T. Amano, in paper RD06 at the 70th International Symposium on Molecular Spectroscopy, Champaign-Urbana, Illinois, 2015.
[34]J. L. Dunham, Phys. Rev. **41**, 713–720 (1932); **41**, 721–731 (1932).
[35]G. Herzberg, *Spectra of Diatomic Molecules* (Van Nostrand, New York, 1950).
[36]R. Rydberg, Z. Phys. **73**, 376 (1931); O. Klein, Z. Phys. **76**, 226 (1932); R. Rydberg, Z. Phys. **80**, 514 (1933); A. L. G. Rees, Proc. Phys. Soc. **59**, 998 (1947).
[37]R. J. Le Roy, "RKR1 2.0: A computer program implementing the first-order RKR method for determining diatomic molecule potential energy curves," University of Waterloo Chemical Physics Research Report CP-657, 2003, see http://leroy.uwaterloo.ca/programs/.
[38]R. J. Le Roy and J. van Kranendonk, J. Chem. Phys. **61**, 4750 (1974).
[39]W. M. Kosman and J. Hinze, J. Mol. Spectrosc. **56**, 93 (1975).
[40]C. R. Vidal and H. Scheingraber, J. Mol. Spectrosc. **65**, 46 (1977).
[41]J. A. Coxon and P. G. Hajigeorgiou, J. Mol. Spectrosc. **150**, 1 (1991).
[42]G. Diaz, F. M. Fernández, and E. A. Castro, Chem. Phys. **157**, 35 (1991).
[43]R. Brühl, J. Kapetanakis, and D. Zimmermann, J. Chem. Phys. **94**, 5865 (1991).
[44]J. A. Coxon and P. G. Hajigeorgiou, Can. J. Phys. **70**, 40 (1992).

This article is copyrighted as indicated in the article. Reuse of AIP content is subject to the terms at: http://scitation.aip.org/termsconditions. Downloaded to IP: 129.97.80.15 On: Wed, 13 Jan 2016 18:34:46

[45]H. G. Hedderich, M. Dulick, and P. F. Bernath, J. Chem. Phys. **99**, 8363 (1993).
[46]A. Šurkus, Chem. Phys. Lett. **279**, 236 (1997).
[47]E. G. Lee, J. Y. Seto, T. Hirao, P. F. Bernath, and R. J. Le Roy, J. Mol. Spectrosc. **194**, 197 (1999).
[48]C. Samuelis, E. Tiesinga, T. Laue, M. Elbs, H. Knöckel, and E. Tiemann, Phys. Rev. A **63**, 012710 (2000).
[49]A. Pashov, W. Jastrzębski, and P. Kowalczyk, Comput. Phys. Commun. **128**, 622 (2000).
[50]A. Pashov, W. Jastrzębski, and P. Kowalczyk, J. Chem. Phys. **113**, 6624 (2000).
[51]A. Pashov, W. Jastrzębski, W. Jaśniecki, V. Bednarska, and P. Kowalczyk, J. Mol. Spectrosc. **203**, 264 (2000).
[52]H. S. P. Müller, Astron. Astrophys. **514**, L6 (2010).
[53]R. J. Le Roy, J. Seto, and Y. Huang, "`DPotFit 2.0`: A computer program for fitting diatomic molecule spectra to potential energy functions," University of Waterloo Chemical Physics Research Report CP-667, 2013, see http://leroy.uwaterloo.ca/programs/.
[54]R. J. Le Roy and R. B. Bernstein, J. Chem. Phys. **54**, 5114 (1971).
[55]R. J. Le Roy and W.-K. Liu, J. Chem. Phys. **69**, 3622 (1978).
[56]J. Cernicharo, X.-W. Liu, E. González-Alfonso, P. Cox, M. J. Barlow, T. Lim, and B. M. Swinyard, Astrophys. J., Lett. **483**, 65 (1997).
[57]We are grateful to Professor Takayoshi Amano for bringing this misassignment to our attention.
[58]For photofragment kinetic energy measurements, Helm et al. suggested that the uncertainties for levels with $v' = 0$–4 would be ~9 cm^{-1} and those for $v' > 4$ about 20 cm^{-1} and also that there was a ±10% uncertainty in the raw kinetic energy measurements. For simplicity, the present work used 10% of measured energy as the uncertainty for reported kinetic energies larger than 200 cm^{-1}, and 20 cm^{-1} for the smaller values.
[59]A. L. Cooksy, G. A. Blake, and R. J. Saykally, Astrophys. J. **305**, L89 (1986).
[60]S. Walji, K. M. Sentjens, and R. J. Le Roy, J. Chem. Phys. **142**, 044305 (2015).
[61]V. V. Meshkov, A. V. Stolyarov, M. C. Heaven, C. Haugen, and R. J. Le Roy, J. Chem. Phys. **140**, 064315 (2014).
[62]R. D. E. Henderson, A. Shayesteh, J. Tao, C. C. Haugen, P. F. Bernath, and R. J. Le Roy, J. Phys. Chem. A **117**, 13373 (2013).
[63]T. Yukiya, N. Nishimiya, Y. Samajima, K. Yamaguchi, M. Suzuki, C. D. Boone, I. Ozier, and R. J. Le Roy, J. Mol. Spectrosc. **283**, 32 (2013).
[64]R. J. Le Roy, J. Mol. Spectrosc. **194**, 189 (1999).
[65]R. J. Le Roy and Y. Huang, J. Mol. Struct.: THEOCHEM **591**, 175 (2002).
[66]J. K. G. Watson, J. Mol. Spectrosc. **80**, 411 (1980).
[67]J. K. G. Watson, J. Mol. Spectrosc. **223**, 39 (2004).
[68]Y. Huang and R. J. Le Roy, J. Chem. Phys. **119**, 7398 (2003); Erratum, **126**, 169904 (2007).
[69]R. J. Le Roy, N. Dattani, J. A. Coxon, A. J. Ross, P. Crozet, and C. Linton, J. Chem. Phys. **131**, 204309 (2009).
[70]R. J. Le Roy, "Determining equilibrium structures and potential energy functions for diatomic molecules," in *Equilibrium Structures of Molecules*, edited by J. Demaison and A. G. Csaszar (Taylor & Francis, London, 2011), Chap. 6, pp. 159–203.
[71]R. J. Le Roy, C. C. Haugen, J. Tao, and H. Li, Mol. Phys. **109**, 435 (2011).
[72]R. J. Le Roy, Y. Huang, and C. Jary, J. Chem. Phys. **125**, 164310 (2006).
[73]R. J. Le Roy and R. D. E. Henderson, Mol. Phys. **105**, 663 (2007).
[74]H. Salami, A. J. Ross, P. Crozet, W. Jastrzebski, P. Kowalczyk, and R. J. Le Roy, J. Chem. Phys. **126**, 194313 (2007).
[75]G. Lach and N. S. Dattani, private communication (2015).
[76]N. Dattani and R. J. Le Roy, J. Mol. Spectrosc. **268**, 199 (2011).
[77]Our previous work[60–63] used only the much "gentler" constraint that $p_{ad} > m_1$, but that did not force the effective adiabatic potentials $V_{ad}^{(\alpha)}(r)$ for all isotopologues to have exactly the same long-range tail.
[78]R. P. Saxon, K. Kirby, and B. Liu, J. Chem. Phys. **73**, 1873 (1980).
[79]S. P. A. Sauer and V. Špirko, J. Chem. Phys. **138**, 024315 (2013).
[80]Z. Biglari, A. Shayesteh, and A. Maghari, Comput. Theor. Chem. **1047**, 22 (2014).
[81]See supplementary material at http://dx.doi.org/10.1063/1.4939274 for full lists of all the experimental data used in the analysis and of the `[calc.-obs.]` values from the final fit, tables of band constants for all vibrational levels of all isotopologues supported by our potentials, including those for the unobserved tritium species, a Fortran subroutine for generating the effective adiabatic potential of all isotopologues in both states, and sample input data files for using our potentials in the "industry standard" bound-state Franck-Condon factor program LEVEL.[96]
[82]J. A. Coxon, J. Mol. Spectrosc. **152**, 274 (1992).
[83]J. A. Coxon and R. Colin, J. Mol. Spectrosc. **181**, 215 (1997).
[84]J. A. Coxon and P. G. Hajigeorgiou, J. Mol. Spectrosc. **193**, 306 (1999).
[85]R. J. Le Roy, D. R. T. Appadoo, K. Anderson, A. Shayesteh, I. E. Gordon, and P. F. Bernath, J. Chem. Phys. **123**, 204304 (2005).
[86]J. A. Coxon and T. C. Melville, J. Mol. Spectrosc. **235**, 235 (2006).
[87]J. A. Coxon and P. G. Hajigeorgiou, J. Phys. Chem. A **110**, 6261 (2006).
[88]R. J. Le Roy, J. A. Coxon, M. Rey, and V. G. Tyuterev, J. Mol. Spectrosc. **238**, 260 (2006).
[89]A. Shayesteh, R. D. E. Henderson, R. J. Le Roy, and P. F. Bernath, J. Phys. Chem. A **111**, 12495 (2007).
[90]J. A. Coxon and P. G. Hajigeorgiou, J. Quant. Spectrosc. Radiat. Transfer **151**, 133 (2015).
[91]N. S. Dattani, R. J. Le Roy, G. Lach, and L. C. M. Li Chun Fong, in paper MF13 at the 70th International Symposium on Molecular Spectroscopy, University of Illinois, Urbana-Champaign, Illinois, 22-26 June 2015.
[92]Y.-S. Cho, N. S. Dattani, and R. J. Le Roy, in paper MF08 at the 70th International Symposium on Molecular Spectroscopy, University of Illinois, Urbana-Champaign, Illinois, 22-26 June 2015.
[93]One remaining troubling point is the fact that the residual discrepancies for the $R(1)$ microwave transitions of Yu *et al.*, among the most precise of all the 1259 data used in this analysis, have discrepancies 5–6 times their estimated uncertainties. However, the other eight of their 10 data have more acceptable discrepancies (see supplementary material[81]), so we attribute these outliers to a problem in estimating the uncertainties in these data.
[94]R. J. Le Roy, J. Mol. Spectrosc. **191**, 223 (1998).
[95]R. J. Le Roy, J. Chem. Phys. **101**, 10217 (1994).
[96]R. J. Le Roy, "LEVEL 8.2: A computer program for solving the radial Schrödinger equation for bound and quasibound levels," University of Waterloo Chemical Physics Research Report CP-663, 2014, see http://leroy.uwaterloo.ca/programs/.
[97]D. Cerny, R. Bacis, S. Churassy, D. Inard, M. Lamrini, and M. Nota, Chem. Phys. **216**, 207 (1997).
[98]M. M. Graff and J. T. Moseley, Chem. Phys. Lett. **83**, 87 (1981).
[99]K. P. Huber and G. Herzberg, *Constants of Diatomic Molecules* (Van Nostrand Reinhold, New York, 1979).
[100]Ğ. Barinovs and M. C. van Hemert, Chem. Phys. Lett. **399**, 406 (2004).
[101]A. W. Kanzler, H. Sun, and K. F. Freed, Int. J. Quantum Chem. **39**, 269 (1991).
[102]S. Green, P. S. Bagus, B. Liu, A. D. McLean, and M. Yoshimine, Phys. Rev. A **5**, 1614 (1972).

This article is copyrighted as indicated in the article. Reuse of AIP content is subject to the terms at: http://scitation.aip.org/termsconditions. Downloaded to IP: 129.97.80.15 On: Wed, 13 Jan 2016 18:34:46